

Template Synthesis of Iron(II) Complexes Containing Tridentate P–N–S, P–N–P, P–N–N, and Tetradentate P–N–N–P Ligands

Paraskevi O. Lagaditis, Alexandre A. Mikhailine, Alan J. Lough, and Robert H. Morris*

Department of Chemistry, University of Toronto, Toronto, Ontario M5S 3H6 Canada

Received October 2, 2009

A series of mer-tridentate iron(II) complexes bearing P–N–S (**3**), P–N–P (**4**), and P–N–N (**5**) ligands have been prepared via the metal template effect in one pot involving air-stable phosphonium dimers [*cyclo*-(–PPh₂CH₂C(OH)H–)₂](Br)₂ (**1**) and [*cyclo*-(–PCy₂CH₂C(OH)H–)₂](Br)₂ (**2**), KO^tBu, [Fe(H₂O)₆][BF₄]₂ and 2-aminothiophenol (for **3**), 2-(diphenylphosphino)ethylamine (for **4**), and 2-(aminomethyl)pyridine (for **5**). The new phosphonium dimer **2** was prepared via an S_N2 reaction of PCy₂H with BrCH₂CH(OEt)₂. The complexes Fe{PR₂CH₂CH=N(2-C₆H₄)S}₂FeBr₂ (**3a**, R=Ph; **3b**, R=Cy) are paramagnetic, and X-ray diffraction studies revealed that they are bimetallic, in which the S atoms of the bis-tridentate (PNS)₂Fe unit bridge to a FeBr₂ fragment. Complexes [Fe(PR₂CH₂CH=NC₂H₄PPh₂)(NCMe)₃]₂X₂ (**4a**, R=Ph; **4b**, R=Cy; X₂=FeBr₄ or (BF₄)₂) form when 1 equiv of iron is reacted with PPh₂CH₂CH₂NH₂ and 0.5 equiv of the appropriate phosphonium dimer. The evidence for P–N–P coordination is the large ²J_{PP} coupling constant in the ³¹P {¹H} NMR spectrum for the trans phosphorus nuclei. If 0.5 equiv of [Fe(H₂O)₆][BF₄]₂ were added in the synthesis, the complex *trans*-[Fe(NCMe)₂(Ph₂PC₂H₄NH₂)₂][FeBr₄] (**4c**) formed, and this has been characterized by X-ray diffraction. Complexes [Fe{PR₂CH₂CH=NCH₂(2-C₅H₄N)}₂](BPh₄)₂ (**5**) are bis-tridentate iron(II) complexes with pyridyl donors *trans* to the phosphine donors. Interestingly, addition of the diamines ethylenediamine, (1*R*,2*R*)-(–)-1,2-diaminocyclohexane, (1*R*,2*R*)-(–)-1,2-diphenylethylenediamine, or *o*-phenylenediamine, in the template synthesis with **2** led directly to tetradentate P–N–N–P iron(II) complexes *trans*-[Fe(NCMe)₂(PCy₂CH₂CH=N–Q–N=CHCH₂PCy₂)(BPh₄)₂] (Q = CH₂CH₂, **6a**; Q = (1*R*,2*R*)-*cyclo*-C₆H₁₀, **6b**; Q = (1*R*,2*R*)-CHPhCHPh, **6c**; Q = C₆H₄, **6d**). In contrast, similar reactions under the same conditions with dimer **1** led to complexes *mer*-[Fe(P–N–N)₂]²⁺ as reported previously. Complexes **6a** and **6b** have been characterized by X-ray diffraction and exhibited large P–Fe–P bond angles of 112.92(2) and 111.96(4)°, respectively.

Introduction

Polydentate heteroatom ligands, particularly those containing both phosphorus and nitrogen donors, have garnered much attention, as they have been demonstrated to create active catalysts for a multitude of reactions including transfer hydrogenation,^{1–6} direct hydrogenation,^{7–9} cyclopropana-

tion,^{10–12} Michael addition,¹³ oligomerization,^{14,15} and epoxidation.^{10,12} Our group has a particular interest in such complexes with potential activity in the hydrogenation or transfer hydrogenation of polar bonds. Recently, our interest has focused on the P–N–N–P ligand system, and we have reported promising results in the asymmetric transfer hydrogenation of ketones by use of complexes of iron(II) with the general structure shown in Figure 1.^{16–19}

*To whom correspondence should be addressed. E-mail: rmorris@chem.utoronto.ca.

(1) Gao, J.-X.; Zhang, H.; Yi, X.-D.; Xu, P.-P.; Tang, C.-L.; Wan, H.-L.; Tsai, K.-R.; Ikariya, T. *Chirality* **2000**, *12*, 383–388.

(2) Li, Y.-Y.; Zhang, H.; Chen, J.-S.; Liao, X.-L.; Dong, Z.-R.; Gao, J.-X. *J. Mol. Catal. A: Chem.* **2004**, *218*, 153–156.

(3) Clarke, Z. E.; Maragh, P. T.; Dasgupta, T. P.; Gusev, D. G.; Lough, A. J.; Abdur-Rashid, K. *Organometallics* **2006**, *25*, 4113–4117.

(4) Mothes, E.; Sentets, S.; Luquin, M. A.; Mathieu, R.; Lughan, N.; Lavigne, G. *Organometallics* **2008**, *27*, 1193–1206.

(5) Buchard, A.; Heuclin, H.; Auffrant, A.; Goff, X. F. L.; Floch, P. L. *Dalton Trans.* **2009**, 1659–1667.

(6) Gao, J.-X.; Ikariya, T.; Noyori, R. *Organometallics* **1996**, *15*, 1087–1089.

(7) Li, T.; Bergner, I.; Haque, F. N.; Zimmer-De Iulius, M.; Song, D.; Morris, R. H. *Organometallics* **2007**, *26*, 5940–5949.

(8) Rautenstrauch, V.; Hoang-Cong, X.; Churlaud, R.; Abdur-Rashid, K.; Morris, R. H. *Chem.—Eur. J.* **2003**, *9*, 4954–4967.

(9) Diaz-Valenzuela, M. B.; Phillips, S. D.; France, M. B.; Gunn, M. E.; Clarke, M. L. *Chem.—Eur. J.* **2009**, *15*, 1227–1232.

(10) Stoop, R. M.; Bachmann, S.; Valentini, M.; Mezzetti, A. *Organometallics* **2000**, *19*, 4117–4126.

(11) Bonaccorsi, C.; Mezzetti, A. *Organometallics* **2005**, *24*, 4953–4960.

(12) Bonaccorsi, C.; Mezzetti, A. *Curr. Org. Chem.* **2006**, *10*, 225–240.

(13) Hajra, A.; Yoshikai, N.; Nakamura, E. *Org. Lett.* **2006**, *8*, 4153–4155.

(14) Kermagoret, A.; Tomicki, F.; Braunstein, P. *Dalton Trans.* **2008**, 2945–2955.

(15) McGuinness, D. S.; Wasserscheid, P.; Keim, W.; Hu, C.; Englert, U.; Dixon, J. T.; Grove, C. *Chem. Commun.* **2003**, 334–335.

(16) Sui-Seng, C.; Freutel, F.; Lough, A. J.; Morris, R. H. *Angew. Chem., Int. Ed.* **2008**, *47*, 940–943.

(17) Sui-Seng, C.; Haque, F. N.; Hadzovic, A.; Pütz, A.-M.; Reuss, V.; Meyer, N.; Lough, A. J.; Zimmer-De Iulius, M.; Morris, R. H. *Inorg. Chem.* **2009**, *48*, 735–743.

(18) Meyer, N.; Lough, A. J.; Morris, R. H. *Chem.—Eur. J.* **2009**, *15*, 5605–5610.

(19) Mikhailine, A.; Lough, A. J.; Morris, R. H. *J. Am. Chem. Soc.* **2009**, *131*, 1394–1395.

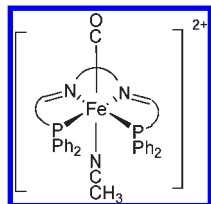
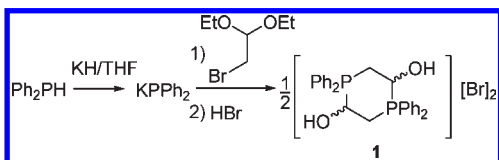


Figure 1. General structure of $trans\text{-}[\text{Fe}(\text{CO})(\text{NCCH}_3)(\text{Ph}_2\text{P-R-HC=N-Q-N=CH-R-PPh}_2)]^{2+}$.

Scheme 1. Synthesis of Dimeric Phosphonium Compound **1**



We have shown that the dimeric phosphonium compound [*cyclo*-($\text{-PPh}_2\text{CH}_2\text{C}(\text{OH})\text{H-}$) $_2$](Br) $_2$ (**1**) is readily prepared in a two-step process where, first, potassium diphenylphosphide is reacted with the commercially available protected aldehyde, 2-bromo-1,1-diethoxyethane ($\text{BrCH}_2\text{CH}(\text{OEt})_2$), and then reacted with $\text{HBr}(\text{aq})$ (Scheme 1). It is a useful precursor for the template synthesis of iron(II) complexes containing tridentate P–N–N or tetradentate P–N–N–P ligands.^{19,20} Depending on which conditions are used, the iron(II) complexes *mer*- $[\text{Fe}(\text{P-N-N})_2]^{2+}$ containing tridentate ligands or *trans*- $[\text{Fe}(\text{NCMe})_2(\text{P-N-N-P})]^{2+}$ containing tetradentate P–N–N–P ligands are formed. The former species forms immediately in acetonitrile, while the latter species either forms slowly in acetonitrile or immediately in methanol with a stoichiometric amount of acetonitrile. In particular, the precursor complex *trans*-(*R,R*)- $[\text{Fe}(\text{CO})(\text{NCCH}_3)(\text{PPh}_2\text{CH}_2\text{CH}=\text{NCHPhCHPhN}=\text{CHCH}_2\text{PPh}_2)]^{2+}$ is a very active and enantioselective ketone transfer hydrogenation catalyst.¹⁹

The template synthesis of these iron(II) complexes is another example where the metal template effect allowed for the synthesis of multidentate ligands that would be otherwise arduous or impossible to obtain using standard organic techniques.^{21–27} The results from the template synthesis approach prompted us in the current work to explore the scope and versatility of the use of such phosphonium dimers in the template synthesis with iron(II) ions. We report here the convenient synthesis of a new dimeric phosphonium compound, **2** (Scheme 2). We show the utility of **1** and **2** in the template synthesis of new iron(II) complexes with bis-tridentate P–N–S, P–N–P, and P–N–N ligands, as well as new iron(II) complexes tetradentate P–N–N–P ligands starting from **2**.

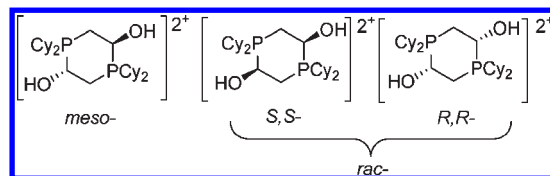
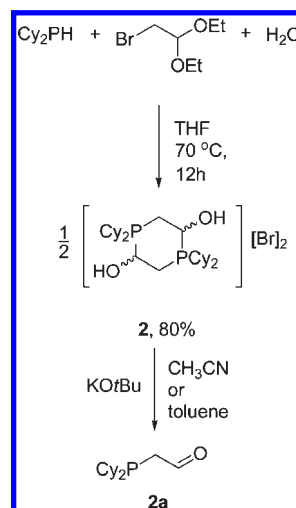


Figure 2. Diastereomers of **2**.

Scheme 2. Preparation of the Phosphonium Dimer, **2**



Results and Discussion

The new dimeric phosphonium compound [*cyclo*-($\text{-PCy}_2\text{-CH}_2\text{C}(\text{OH})\text{H-}$) $_2$](Br) $_2$ (**2**) is synthesized from cyclohexylphosphine (PCy_2H), $\text{BrCH}_2\text{CH}(\text{OEt})_2$, and water in THF in a one-pot reaction. The white, air-stable solid is obtained in a high yield of 80% after the reaction mixture was refluxed overnight (Scheme 2). The synthesis of this dimeric phosphonium compound is simpler than the synthesis of its predecessor, **1**. In the synthesis of **1**, generation of potassium diphenylphosphide, KPPH_2 , from potassium hydride is required because diphenylphosphine, HPPH_2 , is not nucleophilic enough to displace the bromo group on the protected aldehyde. The electron-rich cyclohexyl groups, on the other hand, make the phosphorus center in HPCy_2 more basic and nucleophilic so that the generation of an anion is not required for the $\text{S}_{\text{N}}2$ reaction to proceed.

Like dimer **1**, dimer **2** displays two singlets in the $^{31}\text{P}\{^1\text{H}\}$ NMR spectrum at 27 (major) and 28 (minor) ppm. One of these is due to the presence of the *rac* diastereomer while the other is due to the *meso* diastereomer, although the assignment is not certain, as recrystallization attempts did not separate the two isomers (Figure 2). The ^{31}P NMR chemical shifts of **2** are more downfield than those of **1**, which appear at 12 (major, *rac*) and 17 (minor, *meso*) ppm.²⁸ Furthermore, dimer **2** can be easily cleaved to the phosphine aldehyde (**2a**) under basic conditions, similar to dimer **1**, in either CH_3CN or toluene. An advantage however to toluene is that the KBr salt can be filtered off. The phosphine aldehyde was observed by $^{31}\text{P}\{^1\text{H}\}$ NMR as a singlet at -10 ppm upon the disappearance of the two singlets for **2**. In addition, the ^1H NMR spectrum revealed an aldehyde peak at 9 ppm. The phosphine aldehyde was not isolated

(20) Mikhailine, A. A.; Kim, E.; Dingels, C.; Lough, A. J.; Morris, R. H. *Inorg. Chem.* **2008**, *47*, 6587–6589.

(21) Busch, D. H.; Stephenson, N. A. *Coord. Chem. Rev.* **1990**, *100*, 119–154.

(22) Hoss, R.; Vögtle, F. *Angew. Chem., Int. Ed.* **1994**, *33*, 375–384.

(23) Edwards, P. G.; Malik, K. M. A.; Ooi, L.-I.; Price, A. J. *Dalton Trans.* **2006**, 433–441.

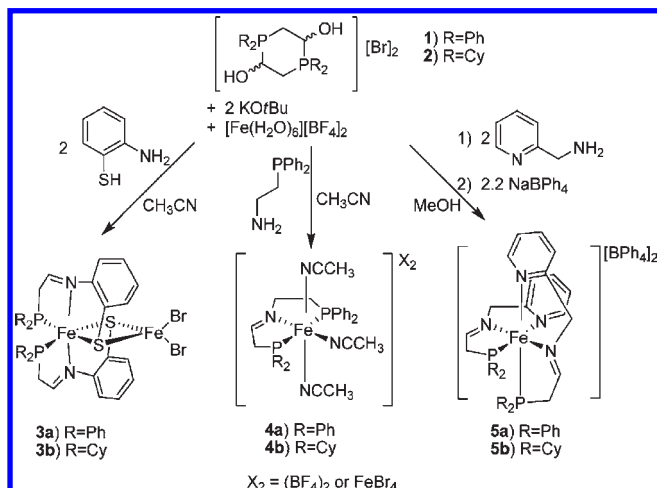
(24) Edwards, P. G.; Haigh, R.; Li, D.; Newman, P. D. *J. Am. Chem. Soc.* **2006**, *128*, 3818–3830.

(25) Kaufhold, O.; Flores-Figueroa, A.; Pape, T.; Hahn, F. E. *Organometallics* **2009**, *28*, 896–901.

(26) Kaufhold, O.; Stasch, A.; Pape, T.; Hepp, A.; Edwards, P. G.; Newman, P. D.; Hahn, F. E. *J. Am. Chem. Soc.* **2009**, *131*, 306–317.

(27) Hahn, F. E.; Klusmann, D.; Pape, T. *Eur. J. Inorg. Chem.* **2008**, 4420–4424.

(28) Matt, D.; Ziessel, R.; DeCian, A.; Fischer, J. *New J. Chem.* **1996**, *20*, 1257–1263.

Scheme 3. Template Synthesis of Novel Bis-Tridentate Iron (II) Complexes with P–N–S, P–N–P, and P–N–N Ligands

but generated in situ for subsequent template synthesis reactions.

The one-pot template reaction of either dimer **1** or **2** with KOtBu, [Fe(H₂O)₆][BF₄]₂ and 2-aminothiophenol gave the air-sensitive, neutral, iron(II) complexes with P–N–S ligands, *mer*-Fe{(C₆H₅)₂PCH₂CH=N(2-C₆H₄)S}₂FeBr₂ (**3a**) and *mer*-Fe{(C₆H₁₁)₂PCH₂CH=N(2-C₆H₄)S}₂FeBr₂ (**3b**), respectively (Scheme 3). The burgundy-colored complexes **3a** and **3b** precipitated out of the reaction mixture and were isolated in yields of 57% and 60%. Both complexes were insoluble in common organic solvents but were completely soluble in dimethylsulfoxide (DMSO) or dimethyl formamide (DMF); they were slightly soluble in alcohols but decompose over time, as noted by the change in color from burgundy to yellow-brown.

The structures of **3a** and **3b** were first believed to be *mer*-Fe(P–N–S)₂, as the corresponding monocationic complexes were observed in the electrospray ionization (ESI⁺) mass spectra. The growth of crystals of **3a** and **3b** proved to be challenging, as the solvent choice was limited. Nonetheless, crystals of **3a** were grown from a reaction mixture by slow diffusion of 2-aminothiophenol in acetonitrile to an acetonitrile mixture of dimer **1**, KOtBu, and [Fe(H₂O)₆][BF₄]₂ (Figure 3). The X-ray crystal structure of **3a** was not just the Fe(P–N–S)₂ complex but a bimetallic species with bridging thiolate groups. The structure of **3a** in Figure 3 is C₂-symmetric. The iron(II) ion, Fe(1), that is coordinated to the P–N–S ligands, is pseudo-octahedral, while the second iron(II) center, Fe(2), is pseudo-tetrahedral. The Br–Fe(2)–Br bond angle of 109.24° is correct for a perfect tetrahedral geometry; however, the S–Fe(2)–S bond angle of 91.77° is smaller due the rigidity of the P–N–S ligand. The bridging S atoms form almost a perfect Fe₂S₂ square in which the imperfection is due to the slight difference in bond lengths between the two iron centers. In addition, the Fe₂S₂ unit is perfectly planar.

The formation of the complexes **3** may proceed via a thiazolidine intermediate. A thiazolidine is known to form

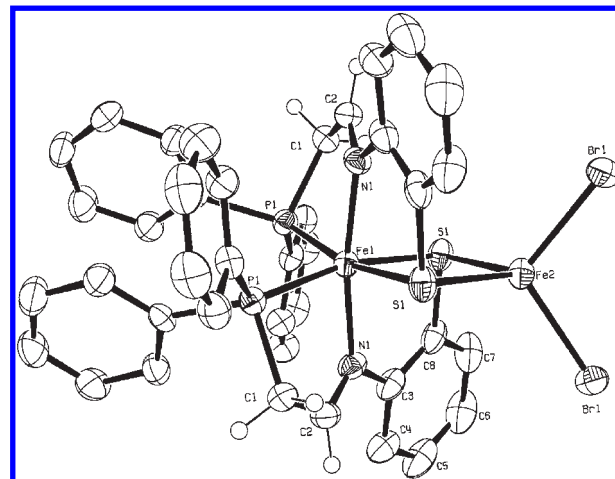


Figure 3. ORTEP plot (50% probability ellipsoids) of the X-ray crystal structure of **3a**. Hydrogen atoms are omitted for clarity. Selected bond lengths (Å) and angles (deg): Fe(1)–S(1), 2.3540(10); Fe(2)–S(1), 2.3811(10); Br(1)–Fe(2), 2.4139(6); Fe(1)–P(1), 2.2349(10); Fe(1)–N(1), 1.993(3); N(1)–Fe(1)–N(1), 170.57(17); P(1)–Fe(1)–P(1), 97.98(5); S(1)–Fe(1)–S(1), 93.13(5); S(1)–Fe(2)–S(1), 91.77(5); Br(1)–Fe(2)–Br(1), 109.24(3); Fe(1)–S(1)–Fe(2), 87.55(3).

in the reaction between *o*-(diphenylphosphino)benzaldehyde and 2-aminothiophenol.^{29–31} A ³¹P{¹H} NMR test sample containing a mixture of **1** or **2** with a base and 2-aminothiophenol revealed a major peak at 50 ppm. The generation of FeBr₄^{2–} is crucial since reactions carried out in a toluene/acetonitrile solvent mixture to exclude bromide salts from the solution did not produce the same results. Hence, FeBr₄^{2–} may ring-open the thiazolidine intermediate to give complexes **3a** and **3b**.

Complexes **3** are paramagnetic and could not be characterized by NMR spectroscopy. The solid-state room-temperature magnetic moment was determined to be 5.02 μ_B for **3a** and 5.06 μ_B for **3b** with corrections for diamagnetism. These values are close to the spin-only value for four unpaired electrons (4.9 μ_B) and imply that there is a high-spin iron(II) center. It is most likely that the tetrahedral iron center, Fe(2), is high-spin, while the iron center that is coordinated by the P–N–S ligands, Fe(1), in an octahedral fashion is low-spin. The electronic spectrum of a DMSO solution (10^{–4} M) of **3a** shows two charge transfer transitions at 310 (ε = 15 933 M^{–1} cm^{–1}) and 523 nm (ε = 762 M^{–1} cm^{–1}), while that of **3b** shows two transitions at 306 (ε = 7558 M^{–1} cm^{–1}) and 540 nm (ε = 1547 M^{–1} cm^{–1}).

The cyclic voltammetry of **3a** and **3b** revealed the non-innocent behavior of ligands containing S donors.^{32–34} Figure 4 shows the cyclic voltammogram of **3a** and **3b** in DMF; for **3b**, two cathodic signals at 0.70 and 0.11 V with corresponding anodic signals, 0.60 and 0.07 V, respectively, are assigned to the Fe³⁺/Fe²⁺ redox couple of both iron centers. The very sharp anodic signal (–0.28 V) and broad cathodic signal (–0.67 V) are from the redox couple of the P–N–S ligand. The cyclic voltammogram of **3a** shows the

(31) Castiñeiras, A.; Gómez, M. C.; Sevillano, P. *J. Mol. Struct.* **2000**, 554, 301–306.

(32) Ghosh, P.; Begum, A.; Herebian, D.; Bothe, E.; Hildenbrand, K.; Weyhermüller, T.; Wieghardt, K. *Angew. Chem., Int. Ed.* **2003**, 42, 563–567.

(33) Ghosh, P.; Begum, A.; Bill, E.; Weyhermüller, T.; Wieghardt, K. *Inorg. Chem.* **2003**, 42, 3208–3215.

(34) Roy, N.; Sproules, S.; Weyhermüller, T.; Wieghardt, K. *Inorg. Chem.* **2009**, 48, 3783–3791.

(29) Dilworth, J. R.; Howe, S. D.; Hutson, A. J.; Miller, J. R.; Silver, J.; Thompson, R. M.; Harman, M.; Hursthouse, M. B. *J. Chem. Soc., Dalton Trans.* **1994**, 3553–3564.

(30) Bayly, S. R.; Cowley, A. R.; Dilworth, J. R.; Ward, C. V. *Dalton Trans.* **2008**, 2190–2198.

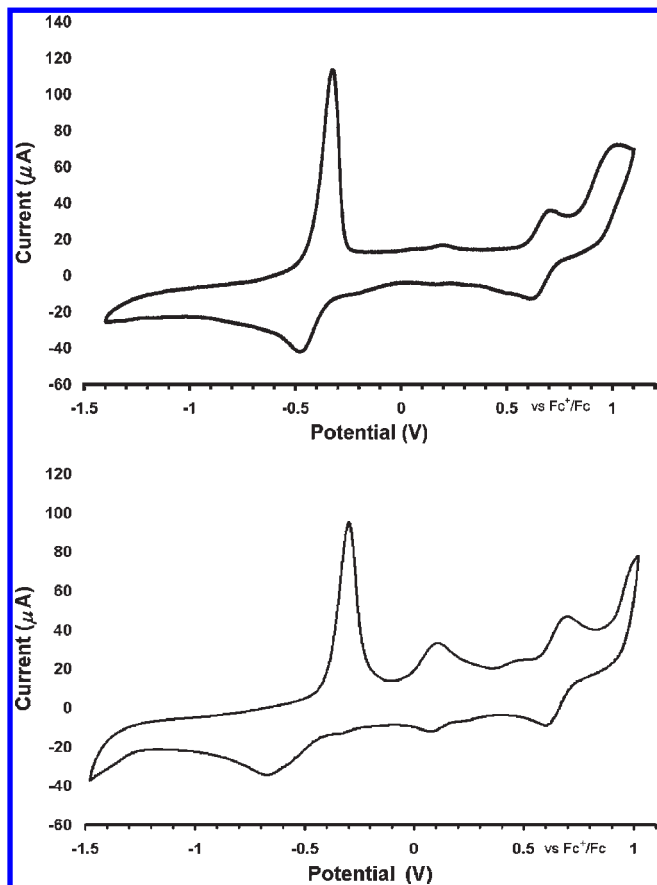


Figure 4. Cyclic voltammogram of **3a** (top) and **3b** (bottom) in DMF solution with 0.1 M [ⁿBu₄N][BF₄] under Ar, scan rate: 50 mV s⁻¹.

same sharp anodic (−0.33 V) and broad cathodic (−0.48 V) signals of the P–N–S ligand redox couple. However, only one Fe³⁺/Fe²⁺ redox couple is observed at 0.71 and 0.61 V.

Changing the amine reagent in the template synthesis to 2-(diphenylphosphino)ethylamine (dpea) led to iron(II) complexes featuring a P–N–P ligand, [Fe{(C₆H₅)₂PCH₂CH=NC₂H₄P(C₆H₅)₂}(NCCH₃)₃]²⁺ (**4a**) and [Fe{(C₆H₁₁)₂PCH₂CH=NC₂H₄P(C₆H₅)₂}(NCCH₃)₃]²⁺ (**4b**) (Scheme 3). Both counteranions, FeBr₄²⁻ and BF₄⁻, exist in the crude product, as observed in the mass spectrum (ESI⁻), when the reaction is carried out in acetonitrile. Attempts to isolate **4a** and **4b** as the tetraphenylborate (BPh₄⁻) salts failed, as these complexes decompose in alcohol solvents; thus, they were simply isolated from CH₂Cl₂ and Et₂O. As a result, complexes **4** were not characterized by elemental analysis since both BF₄⁻ and FeBr₄²⁻ anions coexist in an unknown ratio.

Complexes **4** were characterized by mass spectrometry (ESI⁺), NMR spectroscopy, and IR spectroscopy. The mass spectra of complex **4a** and **4b** both showed peaks with the mass for the monoprotonated tridentate ligand (440.2 and 452.2 *m/z*, respectively). The ³¹P{¹H} NMR spectra of both complexes in acetonitrile-*d*₃ showed two AB doublets at 58.5 and 64.6 ppm for **4a** and 56.6 and 66.6 ppm for **4b**. The doublets of both complexes exhibited large ²*J*_{PP} coupling of 160 and 148 Hz, respectively. The large ²*J*_{PP} coupling and the planar geometry of imine bonds strongly support a mer arrangement of the P–N–P ligand, instead of a fac arrangement, about the iron(II) center. This type of splitting pattern would support only one P–N–P' ligand coordinated to the Fe center. If complexes **4** were bis-tridentate P–N–P' iron-

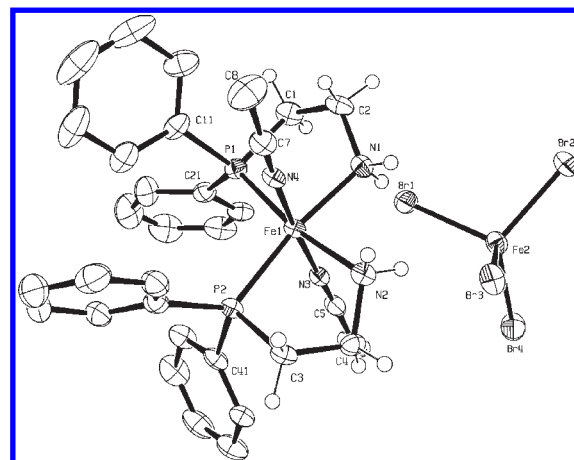
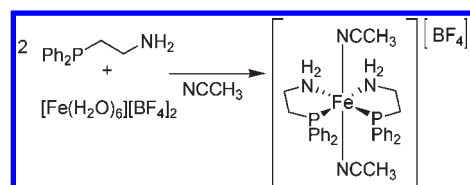


Figure 5. ORTEP plot (30% probability ellipsoids) of the X-ray crystal structure of **4c** as the FeBr₄ salt.

Scheme 4. Synthesis of **4c**

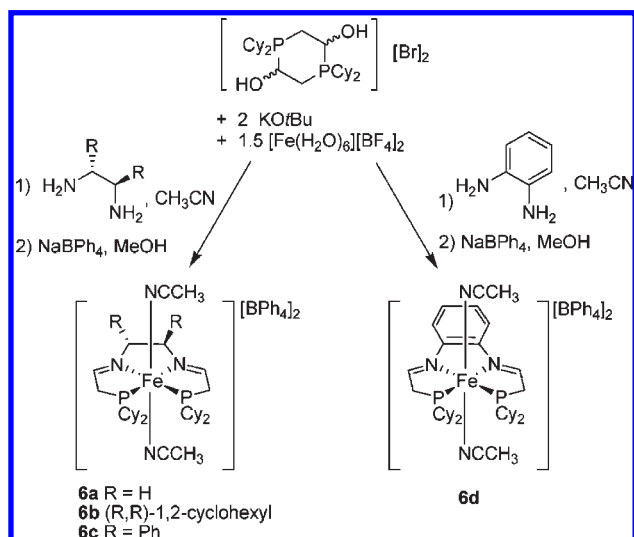


(II) complexes, then both cis and trans couplings should have been observed between each inequivalent P center to produce a second-order AA'XX' splitting pattern. The IR spectra of complexes **4a** and **4b** show an intense stretch at 2203 and 2208 cm⁻¹, respectively. In the case of **4a**, an additional, less intense stretch is present at 2280 cm⁻¹. Typical stretches for coordinated NCCH₃ ligands fall in the range from 2250 to 2290 cm⁻¹; the observed lower frequencies indicated the strongly Lewis acidic character of the iron center.^{16,35} Thus, even without the evidence of X-ray diffraction studies, complexes **4** are concluded to have only one P–N–P and three NCCH₃ ligands coordinated to iron(II), as drawn in Scheme 3.

The ³¹P{¹H} NMR spectra of impure samples of complexes **4a** and **4b** revealed an additional singlet with the same chemical shift at 66.8 ppm. This corresponded to a secondary product, a new complex, *trans*-[Fe(NCMe)₂(Ph₂PC₂H₄NH₂)₂][FeBr₄] (**4c**), which was isolated as a crystal from an NMR sample of crude **4a** in acetonitrile-*d*₃ and characterized by an X-ray diffraction study (Figure 5). This species was isolated as the FeBr₄²⁻ salt from experiments where KBr was not removed. This complex can be obtained as the BF₄⁻ salt by mixing [Fe(H₂O)₆][BF₄]₂ with 2 equiv of dpea in acetonitrile (Scheme 4). A ³¹P{¹H} NMR spectrum of the reaction mixture gave the same singlet as previously observed in the reaction mixture of **4**. Since **4c** is simply the self-assembly of Fe²⁺ and dpea, it will always form in the template synthesis of complexes **4**. In order to avoid or limit **4c**, an excess of Fe²⁺ is required and a ³¹P{¹H} NMR spectrum of the reaction mixtures revealed full conversion to complexes **4**.

By further changing the amine reagent to 2-(aminomethyl)pyridine, the bis-tridentate iron(II) complexes featuring

(35) Benito-Garagorri, D.; Becker, E.; Wiedermann, J.; Lackner, W.; Pollak, M.; Mereiter, K.; Kisala, J.; Kirchner, K. *Organometallics* **2006**, *25*, 1900–1913.

Scheme 5. Template Synthesis of Novel *trans*-Acetonitrile Tetradentate P–N–N–P Iron(II) Complexes from **2**

P–N–N ligands, *mer*-[Fe{(C₆H₅)₂PCH₂HC=NCH₂(C₅H₄-N)}₂]²⁺ (**5a**) and *mer*-[Fe{(C₆H₁₁)₂PCH₂HC=NCH₂(C₅H₅-N)}₂]²⁺ (**5b**), are formed (Scheme 3). Unlike the synthesis of the previous complexes **3** and **4**, the template synthesis of **5a** and **5b** is carried out in methanol rather than acetonitrile because the latter solvent gave multiple products as determined by ³¹P{¹H} NMR spectroscopy. The ³¹P{¹H} NMR spectra showed only a singlet at 62.5 for **5a** and 50.9 for **5b** when the reaction was conducted in methanol. Both complexes were isolated as the BPh₄ salt via a counteranion metathesis with NaBPh₄ in methanol in yields of 82 and 62% for **5a** and **5b**, respectively. The mass spectrum (ESI⁺) provided support for a *bis*-tridentate iron complex, as clusters of the dicationic complex were observed (see the Experimental Section). Crystals of **5a** were grown by the slow diffusion of Et₂O into a MeOH/MeCN (1:1 by volume) solution but were not of good quality for an X-ray diffraction study because they tended to twin. Nonetheless, the X-ray diffraction data supported a *mer*-octahedral arrangement of the P–N–N ligands about iron, as expected and observed in similar complexes with P–N–N ligands either involving a terminal pyridine or amine (–NH₂) donor.^{20,36} Unlike complexes **4**, complexes **5** are very stable in solution under an inert atmosphere and have considerable stability in the solid state in the air, with minimal decomposition after a week.

Although complexes **5** are analogous in structure, a drastic difference between them is their color, owing to the substituents on the P atoms. Complex **5a** is red-pink, while **5b** is dark purple, which indicates that the Ph groups stabilize orbitals of complex **5a** such that the wavelengths of absorbance are significantly blue-shifted. This effect is the most pronounced for complexes **5**, as the color difference between the Cy and Ph analogues of complexes **3** and **4** were merely a difference in the shade of color they exhibited. The electronic spectra of complexes **5** (10^{−4} M) in acetonitrile both display an absorption at 351 (ε = 9822 M^{−1} cm^{−1}) and 358 (ε = 6833 M^{−1} cm^{−1}) nm for **5a** and **5b**, respectively. However, **5a** displayed only

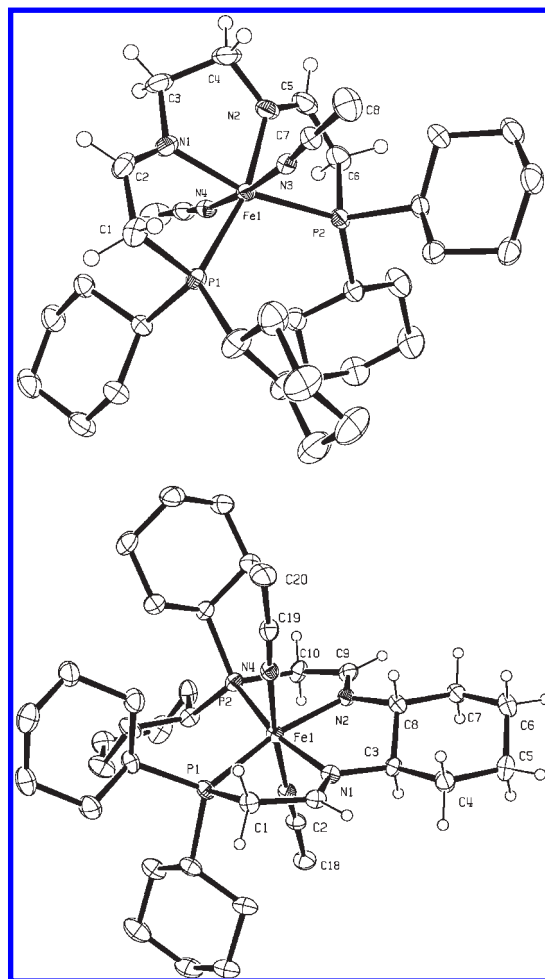


Figure 6. ORTEP plot (30% probability ellipsoids) of the X-ray crystal structures of **6a** (top) and **6b** (bottom). BPh₄[−] and BF₄[−] anions and some hydrogen atoms are omitted for clarity. Selected bond lengths (Å) and angles (deg): for **6a**, Fe(1)–N(1), 1.9643(19); Fe(1)–N(2), 1.966(2); Fe(1)–N(3), 1.932(2); Fe(1)–N(4), 1.921(2); Fe(1)–P(1), 2.2699(7); Fe(1)–P(2), 2.2781(18); N(1)–Fe(1)–N(2), 82.99(9); N(3)–Fe(1)–N(4), 173.65(8); P(1)–Fe(1)–P(2), 112.92(2); for **6b**, Fe(1)–N(1), 1.971(3); Fe(1)–N(3), 1.928(3); Fe(1)–N(4), 1.911(3); Fe(1)–P(1), 2.2936(11); Fe(1)–P(2), 2.2752(10); N(1)–Fe(1)–N(2), 82.73(13); N(4)–Fe(1)–N(3), 174.44(13); P(2)–Fe(1)–P(1), 111.96(4).

one additional charge transfer absorption at 500 (ε = 1483 M^{−1} cm^{−1}), while **5b** displayed two additional, more intense charge transfer absorptions at 510 (ε = 7930 M^{−1} cm^{−1}) and 561 (ε = 8308 M^{−1} cm^{−1}) nm.

Changing the amine reagent in the template reaction from 2-(aminomethyl)pyridine to a diamine, ethylenediamine (en), (1*R*,2*R*)-(–)-1,2-diaminocyclohexane (dach), (1*R*,2*R*)-(–)-1,2-diphenylethylenediamine (dpen), or *o*-phenylenediamine (bn), in acetonitrile, led to a tetradentate ligand complex instead of the bis-tridentate ligand complex. This leads to the direct synthesis of the new tetradentate P–N–N–P iron(II) complexes, *trans*-[Fe{(C₆H₁₁)₂PCH₂CH=NCH₂CH₂N=CHCH₂P(C₆H₁₁)₂}(CH₃CN)₂]²⁺ (**6a**), *trans*-(*R,R*)-[Fe{(C₆H₁₁)₂PCH₂CH=N(C₆H₁₀)N=CHCH₂P(C₆H₁₁)₂}(CH₃CN)₂]²⁺ (**6b**), *trans*-(*R,R*)-[Fe{(C₆H₁₁)₂PCH₂CH=NCH(Ph)CH(Ph)N=CHCH₂P(C₆H₁₁)₂}(CH₃CN)₂]²⁺ (**6c**), and *trans*-[Fe{(C₆H₁₁)₂PCH₂HC=N(C₆H₄)N=CHCH₂P(C₆H₁₁)₂}(CH₃CN)₂]²⁺ (**6d**) (Scheme 5), as determined by NMR, mass spectrometry (ESI⁺), elemental analysis, and X-ray diffraction studies.

(36) Pelagatti, P.; Bacchi, A.; Balordi, M.; Caneschi, A.; Giannetto, M.; Pelizzi, C.; Gonsalvi, L.; Peruzzini, M.; Uguzzoli, F. *Eur. J. Inorg. Chem.* **2007**, 162–171.

A single product was always observed at the end of the reaction, as the $^{31}\text{P}\{^1\text{H}\}$ NMR spectra had only a singlet at 68.5, 68.2, 67.5, and 67.3 ppm for **6a**, **6b**, **6c**, and **6d**, respectively. Initial support for the structure of complexes **6** came from mass spectra (ESI⁺) analyses, as only masses of the tetradentate P–N–N–P ligands were observed and no masses for bis-tridentate iron(II) complexes ($[\text{Fe}(\text{P}–\text{N}–\text{N})_2]^{2+}$) or P–N–N ligands were observed. Even if 2 equiv of the diamine were added, the reaction always led directly to complexes **6**. This was not expected since previous templating with **1** in acetonitrile as a solvent immediately led to bis-tridentate P–N–N iron(II) complexes (except in the case with **bn**). Formation of the tetradentate P–N–N–P iron(II) complexes with **1** was much slower in acetonitrile (24 h with reflux) but formed faster in the polar, protic solvent, methanol with a stoichiometric amount of acetonitrile. It is believed that the protic solvent either is involved with the transformation or stabilizes key intermediates.

We believe that, in the template reaction with **2** to produce the tetradentate complexes, **6** proceeds via a bis-tridentate intermediate in a similar fashion to template reactions involving **1**.^{19,20} Support for this speculation first came from reaction mixtures observed before complete conversion in the synthesis of **6c**. A $^{31}\text{P}\{^1\text{H}\}$ NMR spectrum of the reaction mixture after 12 h revealed three peaks at 67.5, 62.7, and –12.8 ppm. The peak at 67.5 ppm corresponded to **6c** and

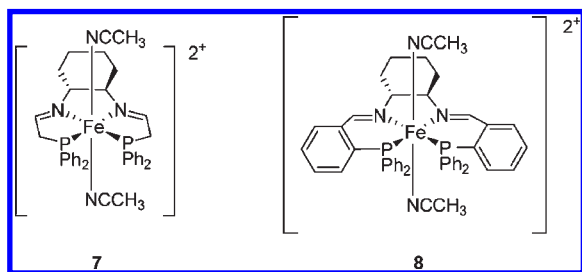


Figure 7. Previous iron(II) complexes with P–N–N–P ligands.

that at –12 ppm to unreacted **2a**. The peak at 62.7 ppm belonged to an intermediate, which fully disappeared after 24 h. This species likely corresponds to a bis-tridentate iron(II) complex. An intermediate has also been observed in a $^{31}\text{P}\{^1\text{H}\}$ NMR spectrum obtained immediately after the addition of **dach** in the synthesis of **6b**. The analogous three peaks were observed at 67.1, 60.2, and –6.7 ppm, where the singlet at 67.1 ppm was assigned to **6b** and –6.7 ppm for **2a**. The peak at 60.2 ppm is again for a similar intermediate species, a bis-tridentate P–N–N iron(II) complex. However, this intermediate species disappeared at a faster rate than the previous intermediate of **6c**. The synthesis of **6c** was the slowest of the four reactions shown in Scheme 5, requiring 24 h for complete conversion at room temperature. This may be a consequence of steric repulsions from the phenyl groups of **dpen** rather than an electron-withdrawing effect since the template synthesis with the least basic of the diamines tested (**bn**) was complete after 12 h. Nevertheless, the synthesis of **6c** is still faster than the synthesis of the analogous complex with **Ph** substituents on the P atoms when carried out under the same conditions.

The fact that tetradentate P–N–N–P iron(II) complexes **6a–d** are formed faster in the template synthesis with **2** than with **1** is a direct consequence of the Cy groups. The Cy groups make the P atoms more basic such that *tert*-butanol (HO*t*Bu), generated in situ upon cleavage of **2**, is a suitable protic source to aid in the transformation from a P–N–N iron(II) complex to a P–N–N–P iron(II) complex.

Complexes **6** were isolated as the BPh₄ salt via a counter-anion metathesis with NaBPh₄ in methanol in yields of 80 (**6a**), 58 (**6b**), 58 (**6c**), and 61% (**6d**). The lower yields of **6b–d** are a consequence of the anion metathesis in methanol, as these complexes are partially soluble in alcohols.

The structures from X-ray diffraction studies of single crystals of **6a** and **6b** are shown in Figure 6. The complexes are distorted octahedral with the acetonitrile ligands in the

Table 1. Selected Crystal Data, Data Collection, and Refinement Parameters for **3a**, **4c**, **6a**, and **6b**

compound	3a	4c [FeBr ₄]	[6a] [BF ₄][BPh ₄]	[6b] [BPh ₄] ₂ ·Et ₂ O
empirical formula	C ₄₀ H ₃₄ Br ₂ Fe ₂ N ₂ P ₂ S ₂	C ₃₄ H ₄₁ Br ₄ Fe ₂ N ₅ P ₂	C ₅₈ H ₈₀ B ₂ F ₄ Fe ₂ N ₄ P ₂	C ₉₀ H ₁₁₆ B ₂ Fe ₂ N ₄ OP ₂
fw	940.27	1012.00	1048.67	1409.28
lattice type	monoclinic	monoclinic	triclinic	orthorhombic
space group	C2/c	P21/c	P1	P212121
T, K	150(1)	150(2)	150(1)	150(1)
a, Å	18.1997(7)	15.4373(4)	11.2526(4)	12.8806(3)
b, Å	14.2222(4)	15.6291(5)	15.1535(5)	20.8835(4)
c, Å	15.3805(6)	18.2926(4)	16.1638(5)	30.1708(7)
α, deg	90	90	96.505(2)	90
β, deg	109.704(2)	106.2720(15)	90.118(2)	90
γ, deg	90	90	90.360(2)	90
V, Å ³	3748.0(2)	4236.7(2)	2738.21(16)	8115.7(3)
Z	4	4	2	4
ρ _{calcd} /Mg m ⁻³	1.666	1.588	1.272	1.153
μ(Mo, Kα), mm ⁻¹	3.136	4.562	0.389	0.273
F(000)	1888	2008	1116	3032
cryst. size, mm ³	0.10 × 0.10 × 0.08	0.22 × 0.16 × 0.12	0.20 × 0.16 × 0.09	0.40 × 0.35 × 0.24
range θ collected, deg	2.56–27.51	2.66–27.51	3.27–27.00	2.57–27.50
reflins collected/unique	15166	25111	32837	37207
abs cor		semiempirical from equivalents		
max and min transmission coeff	0.692 and 0.595	0.577 and 0.441	0.7455 and 0.6221	0.888 and 0.740
goodness of fit	1.052	1.032	1.054	1.021
R ₁ (I > 2σ(I)) ^a	0.0476	0.0463	0.0497	0.0654
wR ₂ (all data) ^a	0.1236	0.1110	0.1377	0.1754
peak and hole, e Å ⁻³	1.346 and –0.618	0.991 and –0.802	1.244 and –0.480	0.677 and –0.455

^a Definition of R indices: $R_1 = \sum(F_o - F_c) / \sum(F_o)$; $wR_2 = [\sum[w(F_o^2 - F_c^2)^2] / \sum[w(F_o^2)^2]]^{1/2}$.

axial positions and the P–N–N–P ligand in the equatorial plane. This mode of coordination has been observed before in analogous iron structures, in particular for comparison purposes *trans*-(*R,R*)-[Fe(NCCH₃)₂{PPh₂CH₂CH=NC₆H₁₀N=CHCH₂PPh₂}]²⁺ (**7**)²⁰ and *trans*-(*R,R*)-[Fe(NCCH₃)₂{PPh₂(*o*-C₆H₄)CH=NC₆H₁₀N=CH(*o*-C₆H₄)PPh₂}]²⁺ (**8**)¹⁶ (Figure 7). Overall, the bond lengths and angles are comparable; however, the most notable structural feature of complexes **6a** and **6b** is the large P–Fe–P bond angles of 112.92 and 111.96°, respectively. A large P–Fe–P angle has also been observed with **7** (109.81°) in comparison to **8** (100.24°). This large angle is a consequence of the five-, five-, and five-membered chelate rings of compound **7** compared to the six-, five-, and six-membered rings of compound **8**. This same geometric constraint exists in complexes **6a** and **6b** since their P–N–N–P ligands form five-, five-, and five-membered chelate rings as well. However, the P–Fe–P angle of complex **6b** is yet slightly larger than **7** due to additional steric strain imposed by the bulky Cy groups on both P atoms.

Regardless of the geometric constraint from the P–N–N–P ligands or the steric bulkiness from the Cy substituents, complexes **6** are stable and do not decompose in the solid state nor in solution under an inert atmosphere. They can be manipulated in the air for short periods of time. Complexes **6a–c** exhibit analogous electronic spectra, which is not surprising since there is little variation in the structure and bonding of the three complexes. Solutions of all three complexes (10^{−4} M) displayed a charge transfer transition at 328 nm ($\epsilon = 3348$ (**6a**), 2952 (**6b**), and 3397 (**6c**) M^{−1} cm^{−1}) and a second, less intense transition at 487 ($\epsilon = 302$ M^{−1} cm^{−1}), 478 ($\epsilon = 268$ M^{−1} cm^{−1}), and 472 ($\epsilon = 500$ M^{−1} cm^{−1}) for **6a**, **6b**, and **6c**, respectively. Complex **6d**, however, displayed a very different electronic spectrum even though it is structurally the same as **6a–c**. The added conjugation from the *ortho*-phenylene group stabilized molecular orbitals of **6d** such that the second charge transfer transition observed with complexes **6a–c** is gone. As a result, **6d** is orange, while **6a–c** are all pink. Table 1 gives selected crystal data, data collection, and refinement parameters for **3a**, **4c**, **6a**, and **6b**.

Conclusion

We have presented a new phosphonium dimer (**2**) that is conveniently synthesized in a one-pot reaction. We have demonstrated its usefulness, along with the previous phosphonium dimer (**1**), in the template synthesis of novel bis-tridentate iron(II) complexes with P–N–S (**3a** and **3b**) and P–N–N (**5a** and **5b**) as well as monotridentate iron(II) complexes with P–N–P ligands (**4a** and **4b**). On the basis of structural evidence and rationale, the ligands of all three classes form a mer arrangement about the iron center. In the case of complexes **3**, the S donors of the P–N–S ligands bridge to a second iron center that is coordinated to two bromine ions in a tetrahedral arrangement. We speculate that such a species is formed by ring-opening of a thiazolidine intermediate by FeBr₄^{2−} to form complexes **3**. In the case of complexes **4**, no crystals for X-ray diffraction study were possible to obtain, but based on a comparison with the other complexes in this report and in the literature, we deduce a mer arrangement of these P–N–P ligands about iron. A byproduct, *trans*-[Fe(NCMe)₂(Ph₂PC₂H₄NH₂)₂][FeBr₄] (**4c**), was found to form in the reaction mixtures of complexes **4** when a

stoichiometric amount of Fe²⁺ was added; it can be avoided when an excess of Fe²⁺ is added after the template reaction mixture is stirred overnight.

We have demonstrated that, when primary diamines are used in the template synthesis with **2**, *trans*-acetonitrile tetradentate P–N–N–P iron(II) complexes **6** are isolated. Since we have previously shown that mer bis-tridentate iron(II) complexes form in such templated reactions with **1**, we speculate from NMR studies that such iron(II) species do form as intermediates in the template synthesis with **2**, but they transform rapidly to the isolated complexes **6**.

The results of this report demonstrate the scope and versatility of the template synthesis. This useful method has led to active catalysts and novel metal complexes. Exploration of new ligand systems as well as the compatibility of the template synthesis of multidentate P and N donor ligands with other metals is currently ongoing.

Experimental Section

General Comments. All procedures and manipulations involving air-sensitive materials were performed under an argon or nitrogen atmosphere using Schlenk techniques or a glovebox with N₂(g). Solvents were degassed and dried using standard procedures prior to all manipulations and reactions. Deuterated solvents were purchased from Cambridge Isotope Laboratories and degassed and dried over activated molecular sieves prior to use. A phosphonium dimer, **1**, was synthesized following a literature procedure.²⁰ All other reagents used were purchased from commercial sources and utilized without further purifications. NMR spectra were recorded at ambient temperature and pressure using a 400 MHz Varian Gemini [¹H (400 MHz), ¹³C{¹H} (100 MHz), and ³¹P{¹H} (161 MHz)]. The ³¹P NMR spectra were referenced to 85% H₃PO₄ (0 ppm). Electronic spectra were recorded on an Agilent 8453 UV–visible photodiode array spectrometer in an anaerobic quartz cuvette (*d* = 1 cm) in CH₃CN or CH₂Cl₂ (complexes **4**) or DMSO (complexes **3**). Magnetic moments were obtained in the solid state with a Johnson Matthey magnetic susceptibility balance. A Bioanalytical Systems Epsilon electrochemical controller was used for cyclic voltammetry studies. All manipulations were conducted in an inert atmosphere. The electrochemical cell was equipped with a Pt wire working electrode, a tungsten auxiliary electrode, and an Ag/AgCl reference electrode; dimethylformamide solutions were 0.1 M in [ⁿBu₄N][BF₄]. Reported potentials are referenced to the ferrocenium/ferrocene couple versus the standard hydrogen electrode, SHE (0.72 V).³⁷ The elemental analyses were performed at the Department of Chemistry, University of Toronto, on a Perkin-Elmer 2400 CHN elemental analyzer. Some complexes gave a low carbon analysis but acceptable hydrogen and nitrogen contents because of a combustion problem. This was not alleviated by the addition of oxidants such as vanadium pentoxide.

Dicyclohexylphosphinoacetaldehyde Bromide Dimer (2). A Schlenk flask was charged with dicyclohexylphosphine (2.53 g, 0.013 mol) and dry THF (10 mL). Bromoacetaldehyde diethyl acetal (2.50 g, 0.013 mol) was added over the course of 15 min. The mixture was stirred for 1 h, at which time a white precipitate was evident. An excess amount of degassed water (1 mL) was added, and the mixture was allowed to reflux overnight to yield a pristine white sludge. The solid was collected by filtration under air and washed with water (2 × 3 mL) and diethyl ether (2 × 3 mL). Drying in vacuo yielded the phosphonium dimer as an air-stable white powder. Yield: 3.25 g (80%). ¹H NMR (400 MHz, CD₃CN): δ 1.42–2.19 (m, HCy), 2.80 (q), 3.08 (m), 5.39

(37) Barrette, W. C.; Johnson, H. W.; Sawyer, D. T. *Anal. Chem.* **1984**, *56*, 1890–1898.

(dd, $J_{\text{HP}} = 26$ Hz, $J_{\text{HH}} = 4$ Hz), 5.23 (dd, $J_{\text{HP}} = 22$ Hz, $J_{\text{HH}} = 4$ Hz). ^{31}P {H} NMR (121 MHz; CD_3CN): 27.2 (s), 28.1 (s). Anal. Calcd for $\text{C}_{28}\text{H}_{52}\text{O}_2\text{P}_2\text{Br}_2$: C, 52.35; H, 8.16. Found: C, 51.93; H, 8.46. MS (ESI, methanol/water; m/z^+): 241.2 [$\text{C}_{28}\text{H}_{52}\text{O}_2\text{P}_2$] $^{2+}$.

[Fe{(C₆H₅)₂PCH₂CH=N(2-C₆H₄)S}₂FeBr₂} (3a). A vial was charged with **1** (150 mg, 0.243 mmol), KO t Bu (54 mg, 0.485 mmol), and CH₃CN (2 mL). After stirring for 5 min, [Fe(H₂O)₆][BF₄]₂ (122 mg, 0.364 mmol) in CH₃CN (1 mL) was added. The reaction mixture was allowed to stir for 20 min. A solution of 2-aminobenzeneethiol (32 mg, 0.249 mmol) in CH₃CN (1 mL) was added to the reaction mixture and stirred overnight. A burgundy precipitate (**3a**) was collected via filtration, washed with acetonitrile (2 × 3 mL), and dried overnight. Yield: 57% (135 mg). $\mu_{\text{eff}} = 5.02 \mu_{\text{B}}$. MS (ESI, methanol/water; m/z^+): 724.2 [$\text{C}_{40}\text{H}_{34}\text{N}_2\text{P}_2\text{Fe}$] $^{+}$.

[Fe{(C₆H₁₁)₂PCH₂CH=N(2-C₆H₄)S}₂FeBr₂} (3b). The synthesis of **3b** was performed in the same manner as **3a** (**2** (150 mg, 0.233 mmol), KO t Bu (52 mg, 0.467 mmol), [Fe(H₂O)₆][BF₄]₂ (118 mg, 0.350 mmol), and 2-aminothiophenol (59 mg, 0.467 mmol) in CH₃CN (5 mL)). Yield: 65% (150 mg). $\mu_{\text{eff}} = 5.08 \mu_{\text{B}}$. MS (ESI, methanol/water; m/z^+): 748.3 [$\text{C}_{40}\text{H}_{50}\text{N}_2\text{P}_2\text{S}_2\text{Fe}$] $^{+}$.

[Fe{(C₆H₅)₂PCH₂CH=NCH₂CH₂P(C₆H₅)₂}(CH₃CN)₃] $^{2+}$ (**4a**). A vial was charged with **1** (80 mg, 0.1294 mmol), KO t Bu (29 mg, 0.259 mmol), and CH₃CN (2 mL). This white slurry was allowed to stir for 5 min until the slurry turned slightly yellow. To this mixture was added [Fe(H₂O)₆][BF₄]₂ (109 mg, 0.323 mmol) in CH₃CN (5 mL) and the mixture stirred for 20 min. A stock solution of 2-(diphenylphosphino)ethylamine (1.03 mL, 0.257 mmol, 230 mg in 4 mL CH₃CN) was added to the solution. The mixture turned purple immediately and was allowed to stir overnight. An additional 35 mg of [Fe(H₂O)₆][BF₄]₂ was added, and after 3 h the brown-pink mixture was filtered through a pad of Celite to remove a gray precipitate. The solvent was removed, the residue was dissolved in CH₂Cl₂ (1 mL), and Et₂O (10 mL) was added. A pale pink precipitate was collected by filtration and washed with Et₂O (2 × 3 mL). Yield: 130 mg. ^1H NMR (400 MHz, CD₃CN): δ 2.95 (m, 2H, CH₂N), 3.64 (d, 2H, $J_{\text{HP}} = 3.65$ Hz, Ph₂PCH₂CH₂), 4.03 (d, 2H, $J_{\text{HP}} = 4.04$ Hz, Ph₂PCH₂CHN), 7.48–7.79 (m, 20H, HPh), 8.14 (d, 1H, $J_{\text{HP}} = 8.15$ Hz, HC=N). ^{13}C { ^1H } NMR (100 MHz, CD₃CN): δ 26.3 (d, $J_{\text{CP}} = 24.0$ Hz, CH₂N), 38.8 (d, $J_{\text{CP}} = 25.0$ Hz, CH₂CHN), 60.8 (d, $J_{\text{CP}} = 5.6$ Hz, Ph₂PCH₂CH₂), 129.5 (dd, $J_{\text{CP}} = 2.2, 4.4$ Hz, C_{Ph}), 129.9 (dd, $J_{\text{CP}} = 2.2, 3.4$ Hz, C_{Ph}), 130.8 (d, $J_{\text{CP}} = 2.4$ Hz, C_{Ph}), 130.7 (d, $J_{\text{CP}} = 2.4, \text{C}_{\text{Ph}}$), 131.7 (d, $J_{\text{CP}} = 9.4$ Hz, C_{Ph}), 132.2 (d, $J_{\text{CP}} = 10.1$ Hz, C_{Ph}), 179.5 (dd, $J_{\text{CP}} = 2.6, 6.8$ Hz, HC=N). ^{31}P { ^1H } NMR (161 MHz, CD₃CN): δ 57.0 ($J_{\text{PP}} = 160$ Hz), 63.3 ($J_{\text{PP}} = 160$ Hz). IR (KBr, cm⁻¹) 2203 (s, $\nu_{\text{C}=\text{N}}$), 2280 (m, $\nu_{\text{C}=\text{N}}$). MS (ESI, methanol/water; m/z^+): 440.2 [$\text{C}_{28}\text{H}_{28}\text{N}_2\text{P}_2$] $^{+}$.

[Fe{(C₆H₁₁)₂PCH₂CH=NCH₂CH₂P(C₆H₅)₂}(CH₃CN)₃] $^{2+}$ (**4b**). The synthesis of **4b** was performed in the same manner as **4a** (**2** (80 mg, 0.125 mmol), KO t Bu (28 mg, 0.250 mmol), [Fe(H₂O)₆][BF₄]₂ (105 mg, 0.311 mmol), and 2-(diphenylphosphino)ethylamine (0.99 mL of stock solution)). After stirring overnight, an additional 35 mg of Fe(H₂O)₆[BF₄]₂ was added, and the reaction mixture was allowed to stir for 3 h. Upon filtering the solution and removing the solvent, a brick-pink solid was isolated and washed with Et₂O (2 × 3 mL). Yield: 130 mg. ^1H NMR (400 MHz, CD₃CN): δ 1.35–2.40 (m, HCy), 2.93 (m, 2H, CH₂N), 3.28 (d, 2H, $J_{\text{HP}} = 3.51$ Hz, C_Y2PCH₂), 3.76 (d, 2H, $J_{\text{HP}} = 3.26$ Hz, Ph₂PCH₂), 7.58–7.86 (m, 10H, HPh), 8.08 (d, 1H, $J_{\text{HP}} = 8.06$ Hz, HC=N). ^{13}C { ^1H } NMR (100 MHz, CD₃CN): δ 25.8 (C_{Cy}), 27.3 (d, $J_{\text{CP}} = 11.3$ Hz, C_{Cy}), 28.4 (d, $J_{\text{CP}} = 23.9$ Hz, CH₂N), 29.0 (C_{Cy}), 34.5 (d, $J_{\text{CP}} = 20.6$ Hz, CH₂CHN), 35.4 (d, $J_{\text{CP}} = 15.2$ Hz, HC_{Cy}P), 62.2 (d, $J_{\text{CP}} = 6.3$ Hz, Ph₂PCH₂CH₂), 129.5 (d, $J_{\text{CP}} = 9.3$ Hz, C_{Ph}), 130.2 (d, $J_{\text{CP}} = 35.9$ Hz, C_{Ph}), 130.8 (d, $J_{\text{CP}} = 2.3$ Hz, C_{Ph}), 132.3 (d, $J_{\text{CP}} = 9.3, \text{C}_{\text{Ph}}$), 180.8 (dd, $J_{\text{CP}} = 2.3, 6.0$ Hz, HC=N). ^{31}P { ^1H } NMR (161 MHz, CD₃CN): δ 55.8 ($J_{\text{PP}} = 148$ Hz), 65.5 ($J_{\text{PP}} = 148$ Hz). IR (KBr, cm⁻¹) 2208 (s, $\nu_{\text{C}=\text{N}}$). MS (ESI, methanol/water; m/z^+): 452.2 m/z [$\text{C}_{28}\text{H}_{40}\text{NP}_2$] $^{+}$.

trans-[Fe(NCMe)₂(Ph₂PC₂H₄NH₂)₂][BF₄]₂ (**4c**). To a stirring solution of [Fe(H₂O)₆][BF₄]₂ (80 mg, 0.237 mmol) and CH₃CN (5 mL) was added 2-(diphenylphosphino)ethylamine (109 mg, 0.474 mmol) in CH₃CN (1 mL) dropwise. The mixture turned purple immediately and was allowed to stir further for 30 min. The solvent was removed, and the residue was dissolved in CH₂Cl₂ (1 mL). The addition of Et₂O (10 mL) afforded a purple solid, which was isolated by filtration and dried in vacuo. Yield: 93% (170 mg). ^1H NMR (400 MHz, CD₃CN): δ 1.96 (s, CH₃), 2.93 (m, 4H, H₂CP), 3.09 (m, 4H, H₂CN), 3.69 (s, 4H, H₂N), 6.99 (t, 8H, HAr), 7.29 (t, 8H, HAr), 7.49 (t, 4H, HAr). ^{13}C { ^1H } NMR (100 MHz, CD₃CN): δ 31.46 (dd, H₂CP, $J_{\text{CP}} = 14, 14.7$ Hz), 41.56 (m, H₂CN), 129.58 (t, $J_{\text{CP}} = 4.6$ Hz, HC_{Ar}P), 131.29 (m, HC_{Ar}P), 131.78 (dd, $J_{\text{CP}} = 16.9, 19.4$ Hz, C_{Ar}P), 132.83 (t, $J_{\text{CP}} = 4.5$ Hz, HC_{Ar}P). ^{31}P { ^1H } NMR (161 MHz, CD₃CN): δ 64.6 (s). Anal. Calcd for C₃₂H₃₈N₄P₂FeB₂F₄: C, 49.91; H, 4.97; N, 7.28. Found: C, 48.67; H, 5.14; N, 6.42. Crystals of **4c** as the FeBr₄ salt suitable for X-ray diffraction were obtained from a NMR sample of an incomplete reaction of **4a** in acetonitrile-*d*₃.

[Fe{(C₆H₅)₂PCH₂CH=NCH₂(C₅H₄N)}₂][BPh₄]₂ (**5a**). A vial was charged with **1** (80 mg, 0.129 mmol), KO t Bu (29 mg, 0.259 mmol), and MeOH (4 mL). [Fe(H₂O)₆][BF₄]₂ (65 mg, 0.194 mmol) in MeOH (1 mL) was added to the colorless reaction mixture after 5 min. After stirring for 20 min, 0.52 mL of a stock solution of 2-(aminomethyl)pyridine (215 mg in 4 mL of MeOH) was added to the colorless mixture. The mixture first turned yellow, and after stirring overnight, the mixture turned dark pink. The mixture was filtered through a pad of Celite, concentrated (~2 mL) under reduced pressure, and added to a solution of NaBPh₄ (94 mg, 0.275 mmol) in MeOH (1 mL) to cause the formation of a dark pink precipitate. The solid was filtered and washed with MeOH (2 × 1 mL) and dried under a vacuum. Yield: 87% (151 mg). ^1H NMR (400 MHz, CD₃CN): δ 4.05 (d, 2H, HCP), 4.35 (d, 2H, HCP), 5.10 (d, 2H, HC-N), 5.40 (d, 2H, HC-N), 6.84–7.05 (m, 24H, HPh), 7.22 (t, 4H, Hpy), 7.31 (s, 16H, HPh), 7.44 (t, 2H, Hpy), 7.67 (d, 2H, Hpy), 7.83 (d, 2H, HC=N). ^{13}C { ^1H } NMR (100 MHz, CD₃CN): δ 40.53 (dd, $J_{\text{CP}} = 15, 10$ Hz CH₂P), 64.81 (CH₂N), 122.09 (C_{py}), 122.80 (C_{Ph}B), 125.61 (C_{py}), 126.62 (q, C_{Ph}B), 129.56 (C_{Ph}P), 130.09 (C_{Ph}P), 130.46 (C_{Ph}P), 130.66 (C_{Ph}B), 131.89 (C_{Ph}P), 132.02 (C_{Ph}P), 136.75 (q, $J_{\text{CB}} = 1.3$ Hz, C_{Ph}B), 138.56 (C_{py}), 151.21 (C_{py}), 162.01 (C_{py}), 164.81 (m, $J_{\text{CB}} = 49$ Hz, C_{Ph}B), 180.36 (t, $J_{\text{CP}} = 3.5$ Hz, CHN). ^{31}P { ^1H } NMR (161 MHz, CD₃CN): δ 62.51. Anal. Calcd for C₈₈H₇₈N₄P₂FeB₂: C, 79.41; H, 5.91; N, 4.21. Found: C, 71.97; H, 5.37; N, 4.37. MS (ESI, methanol/water; m/z^+): 346.1 [$\text{C}_{40}\text{H}_{38}\text{N}_4\text{P}_2\text{Fe}$] $^{2+}$.

[Fe{(C₆H₁₁)₂PCH₂CH=NCH₂(C₄H₄N)}₂][BPh₄]₂ (**5b**). Following the same procedure as for **5a** (**2** (80 mg, 0.125 mmol), KO t Bu (28 mg, 0.249 mmol), and [Fe(H₂O)₆][BF₄]₂ (63 mg, 0.187 mmol) in MeOH (5 mL)), a solution of 2-(aminomethyl)pyridine (0.50 mL from a stock solution of 215 mg in 4 mL of MeOH) was added to the colorless mixture. The mixture first turned red, and after stirring overnight, the mixture turned purple-black. The mixture was filtered through a pad of Celite, concentrated (~2 mL) under reduced pressure, and added to a solution of NaBPh₄ (94 mg, 0.274 mmol) in MeOH (1 mL) to cause the formation of a purple precipitate. The solid was filtered and washed with MeOH (2 × 1 mL) and dried under a vacuum. Yield: 62% (105 mg). ^1H NMR (400 MHz, CD₂Cl₂): δ 0.91–2.06 (m, HCy), 2.31 (m, 2H, HCP), 3.06 (m, 2H, HC-N), 3.99 (m, 2H, HC-N), 6.77 (s, 2H, Hpy), 6.87 (t, 8H, HPh), 6.96 (d, 2H, Hpy), 7.08 (m, 16H, HPh), 7.27 (t, 2H, Hpy), 7.35 (d, 2H, Hpy), 7.59 (s, 16H, HPh), 7.73 (t, 2H, HC=N). ^{13}C { ^1H } NMR (100 MHz, CD₂Cl₂): δ 26.46 (C_{Cy}), 28.51 (C_{Cy}), 30.24 (C_{Cy}), 30.93 (C_{Cy}), 31.36 (C_{Cy}), 37.88 (C_{Cy}), 41.23 (CH₂P), 57.53 (CH₂N), 122.66 (C_{Ph}B), 126.57 (C_{Ph}B), 126.98 (C_{py}), 129.21 (C_{py}), 136.21 (C_{Ph}B), 138.21 (C_{py}), 149.77 (C_{py}), 158.44 (C_{py}), 164.86 (C_{Ph}B), 171.23 (HC=N). ^{31}P { ^1H } NMR (161 MHz,

CD_2Cl_2): δ 50.03. Anal. Calcd for $\text{C}_{88}\text{H}_{102}\text{N}_4\text{P}_2\text{FeB}_2$: C, 77.99; H, 7.59; N, 4.13. Found: C, 76.74; H, 7.02; N, 4.88. MS (ESI, methanol/water; m/z^+): 358.2 [$\text{C}_{40}\text{H}_{62}\text{N}_4\text{P}_2\text{Fe}$] $^{2+}$.

Precursor Solution A. A vial was charged with **2** (200 mg, 0.311 mmol), KORBu (70 mg, 0.623 mmol), and CH_3CN (4 mL). After stirring for 5 min, $[\text{Fe}(\text{H}_2\text{O})_6][\text{BF}_4]_2$ (158 mg, 0.467 mmol) in CH_3CN (2 mL) was added to the white slurry. The solution turned gray-yellow after 5 min.

***trans*-[Fe{(C₆H₁₁)₂PCH₂CH=NCH₂CH₂N=CHCH₂P(C₆H₁₁)₂}(CH₃CN)₂][BPh₄]₂ (**6a**).** To precursor solution A was added ethylenediamine (0.34 mL from a stock solution of 200 mg in 4 mL of CH_3CN). The mixture turned pink immediately. After the reaction has gone to completion overnight, the mixture was filtered through a pad of Celite to remove a gray-white precipitate. Solvent was removed under reduced pressure to give a red-pink residue. The solid was dissolved in MeOH (2 mL) and added to a solution of NaBPh_4 (234 mg, 0.685 mmol) in MeOH (1 mL) to cause precipitation of a pale pink solid. The solid was filtered and washed with MeOH (2 × 1 mL) and dried under a vacuum. Yield: 80% (319 mg). Single crystals suitable for an X-ray diffraction study were obtained by the slow diffusion of pentane into $\text{CH}_3\text{CN}/\text{CH}_2\text{Cl}_2$ (1:1 by volume) at -40°C . ^1H NMR (400 MHz, CD_3CN): δ 1.11–1.95 (m, *HCy*, *CH*₃), 3.31 (d, 4H, *H*₂CP), 3.95 (s, 4H, *H*₂C–N), 6.8–7.3 (m, *HAr*), 8.41 (m, 2H, *HC=N*). ^{13}C { ^1H } NMR (100 MHz, CD_3CN): δ 26.58 (*C*_{Cy}), 27.63 (t, $J_{\text{CP}} = 5.1$ Hz, *C*_{Cy}), 27.82 (t, $J_{\text{CP}} = 5.1$ Hz, *C*_{Cy}), 29.87 (*C*_{Cy}), 30.04 (*C*_{Cy}), 35.72 (t, $J_{\text{CP}} = 6.9$ Hz, *C*_{Cy}P), 36.92 (dd, $J_{\text{CP}} = 15, 10$ Hz, *CH*₂P), 61.10 (*CH*₂N), 122.61 (*C*_{Ph}B), 126.43 (q, $J_{\text{CB}} = 2.7$ Hz, *C*_{Ph}B), 136.58 (q, $J_{\text{CB}} = 1.4$ Hz, *C*_{Ph}B), 164.62 (m, $J_{\text{CB}} = 49$ Hz, *C*_{Ph}B), 177.86 (*HC=N*). ^{31}P { ^1H } NMR (161 MHz, CD_3CN): δ 68.5 (s). Anal. Calcd for $\text{C}_{82}\text{H}_{100}\text{N}_4\text{P}_2\text{FeB}_2$: C, 76.88; H, 7.87; N, 4.37. Found: C, 71.23; H, 7.51; N, 4.47. MS (ESI, methanol/water; m/z^+): 505.4 [$\text{C}_{30}\text{H}_{55}\text{N}_2\text{P}_2$] $^+$.

***trans*-[Fe{(C₆H₁₁)₂PCH₂CH=N(C₆H₁₀)N=CHCH₂P(C₆H₁₁)₂}(CH₃CN)₂][BPh₄]₂ (**6b**).** A solution of (1*R*,2*R*)-(–)-1,2-diaminocyclohexane (36 mg, 0.311 mmol) in CH_3CN (1 mL) was added to precursor solution A. The color of the reaction mixture turned pink within 5 min. After stirring overnight, the reaction mixture was filtered through a pad of Celite to remove a gray-white precipitate, and the solvent was removed under reduced pressure to give a red-pink residue. The solid was dissolved in MeOH (2 mL) and added to a solution of NaBPh_4 (266 mg, 0.778 mmol) in MeOH (1 mL) to cause precipitation of a pale pink solid. The solid was filtered and washed with MeOH (2 × 1 mL) and dried under a vacuum. Yield: 58% (242 mg). Single crystals suitable for an X-ray diffraction study were obtained by the slow diffusion of Et₂O into MeOH/ CH_3CN (1:1 by volume). ^1H NMR (400 MHz, CD_3CN): δ 1.24–1.95 (m, *HCy*, *CH*₃), 2.53 (d, 2H, *H*_{Cy}P), 3.12 (d, 2H, *H*CP), 3.36 (m, 2H, *HC=N*), 3.49 (m, 2H, *H*CP), 6.8–7.2 (m, *HAr*), 8.35 (m, 2H, *HC=N*). ^{13}C { ^1H } NMR (100 MHz, CD_3CN): δ 24.42 (*C*_{Cy}), 26.31 (*C*_{Cy}), 26.63 (*C*_{Cy}P), 27.48 (t, $J_{\text{CP}} = 5.1$ Hz, *C*_{Cy}P), 27.66 (q, $J_{\text{CP}} = 5.1$ Hz, *C*_{Cy}P), 28.86 (*C*_{Cy}), 29.58 (*C*_{Cy}P), 30.35 (*C*_{Cy}), 30.40 (d, $J_{\text{CP}} = 4.6$ Hz, *C*_{Cy}P), 35.50 (q, $J_{\text{CP}} = 2.9$ Hz, *C*_{Cy}P), 36.56 (dd, $J_{\text{CP}} = 10.1, 14.7$ Hz, *CH*₂P), 71.94 (*HC=N*), 122.48 (*C*_{Ph}B), 126.30 (q, $J_{\text{CB}} = 2.8$ Hz, *C*_{Ph}B), 136.44 (q, $J_{\text{CB}} = 1.4$ Hz, *C*_{Ph}B), 163.75–165.22 (m, $J_{\text{CB}} = 49$ Hz, *C*_{Ph}B), 173.87 (*HC=N*). ^{31}P { ^1H } NMR (161 MHz, CD_3CN): δ 68.2 (s). Anal. Calcd for

$\text{C}_{86}\text{H}_{106}\text{N}_4\text{P}_2\text{FeB}_2$: C, 77.36; H, 8.00; N, 4.20. Found: C, 72.68; H, 7.85; N, 4.11. MS (ESI, methanol/water; m/z^+): 559.4 [$\text{C}_{34}\text{H}_{61}\text{N}_2\text{P}_2$] $^+$.

***trans*-[Fe{(C₆H₁₁)₂PCH₂CH=NCH(Ph)CH(Ph)N=CHCH₂P(C₆H₁₁)₂}(CH₃CN)₂][BPh₄]₂ (**6c**).** A solution of (1*R*,2*R*)-(–)-1,2-diphenylethylenediamine (66 mg, 0.311 mmol) in CH_3CN (1 mL) was added to precursor solution A. The mixture slowly turned pink, and after stirring for 48 h, the mixture was filtered through a pad of Celite to remove a gray-white precipitate. The solvent was removed under reduced pressure to give a red-pink residue. The solid was dissolved in MeOH (2 mL) and added to a solution of NaBPh_4 (266 mg, 0.778 mmol) in MeOH (1 mL) to cause the formation of a dark pink precipitate. The solid was filtered and washed with MeOH (2 × 1 mL) and dried under a vacuum. Yield: 58% (260 mg). ^1H NMR (400 MHz, CD_3CN): δ 1.13–2.16 (m, *HCy*, *CH*₃), 3.21 (d, 2H, *H*₂CP), 3.42 (m, 2H, *H*₂CP), 5.30 (s, 2H, *H*CP), 6.86–7.40 (m, *HAr*), 7.88 (m, 2H, *HC=N*). ^{13}C { ^1H } NMR (100 MHz, CD_3CN): δ 26.50 (*C*_{Cy}P), 26.82 (*C*_{Cy}P), 27.77 (q, $J_{\text{CP}} = 5.1$ Hz, *C*_{Cy}P), 27.91 (q, $J_{\text{CP}} = 4.8$ Hz, *C*_{Cy}P), 29.23 (*C*_{Cy}), 29.75 (*C*_{Cy}), 30.56 (*C*_{Cy}), 35.81 (t), 36.00 (t), 36.59 (dd, $J_{\text{CP}} = 10.1, 14.7$ Hz, *CH*₂P), 78.58 (*HC=N*), 122.64 (*C*_{Ph}B), 126.47 (q, $J_{\text{CB}} = 2.7$ Hz, *C*_{Ph}B), 130.26 (*C*_{Ph}), 130.43 (*C*_{Ph}), 130.74 (*C*_{Ph}), 134.41 (*C*_{Ph}), 136.62 (q, $J_{\text{CB}} = 1.3$ Hz, *C*_{Ph}B), 163.94–165.41 (m, $J_{\text{CB}} = 49$ Hz), 178.15 (s, *HC=N*). ^{31}P { ^1H } NMR (161 MHz, CD_3CN): δ 67.5 (s). Anal. Calcd for $\text{C}_{94}\text{H}_{105}\text{N}_4\text{P}_2\text{FeB}_2$: C, 78.77; H, 7.59; N, 3.91. Found: C, 74.92; H, 7.53; N, 3.74. MS (ESI, methanol/water; m/z^+): 657.4 [$\text{C}_{42}\text{H}_{63}\text{N}_2\text{P}_2$] $^+$.

***trans*-[Fe{(C₆H₁₁)₂PCH₂HC=N(C₆H₄)N=CHCH₂P(C₆H₁₁)₂}(CH₃CN)₂][BPh₄]₂ (**6d**).** A solution of *o*-phenylenediamine (14 mg, 0.125 mmol) in CH_3CN (1 mL) was added to precursor solution A. The mixture first turned brown, and after stirring overnight, the mixture became orange. The solvent was removed under reduced pressure to give a red-orange solid. The solid was dissolved in MeOH (2 mL) and added to a solution of NaBPh_4 (94 mg, 0.274 mmol) in MeOH (1 mL) to cause precipitation of an orange solid. The solid was filtered and washed with MeOH (2 × 1 mL) and dried under a vacuum. Yield: 61% (252 mg). ^1H NMR (400 MHz, CD_3CN): δ 1.24–1.95 (m, *HCy*, *CH*₃), 3.66 (d, 4H, *H*₂CP), 6.82–7.28 (m, *HAr*), 7.54 (m, 2H, *HAr*), 7.99 (m, 2H, *HAr*), 9.07 (m, 2H, *HC=N*). ^{13}C { ^1H } NMR (100 MHz, CD_3CN): δ 26.64 (*C*_{Cy}P), 27.93 (t, $J_{\text{CP}} = 4.9$ Hz, *C*_{Cy}P), 28.07 (t, $J_{\text{CP}} = 5.2$ Hz, *C*_{Cy}P), 29.96 (*C*_{Cy}P), 30.23 (*C*_{Cy}P), 36.32 (t, $J_{\text{CP}} = 7$ Hz, *C*_{Cy}P), 37.95 (dd, $J_{\text{CP}} = 10.1, 14.7$ Hz, *CH*₂P), 122.65 (*C*_{Ph}B), 126.47 (q, $J_{\text{CB}} = 2.7$ Hz, *C*_{Ph}B), 130.83 (*C*_{Ph}), 136.61 (m, *C*_{Ph}B), 145.28 (*C*_{Ph}), 164.67 (m, $J_{\text{CB}} = 49$ Hz, *C*_{Ph}B), 175.11 (*HC=N*). ^{31}P { ^1H } NMR (161 MHz, CD_3CN): δ 67.3 (s). Anal. Calcd for $\text{C}_{86}\text{H}_{100}\text{N}_4\text{P}_2\text{FeB}_2$: C, 77.71; H, 7.58; N, 4.22. Found: C, 66.88; H, 6.98; N, 3.50. MS (ESI, methanol/water; m/z^+): 553.4 [$\text{C}_{34}\text{H}_{55}\text{N}_2\text{P}_2$] $^+$.

Acknowledgment. R.H.M. thanks NSERC for a Discovery Grant and the PRF, as administered by the ACS, for an AC grant.

Supporting Information Available: Complete crystallographic data in CIF format for complexes **3a**, **4c**[FeBr_4], **6a**[BPh_4][BF_4], and **6b**[BPh_4]-Et₂O. This material is available free of charge via the Internet at <http://pubs.acs.org>.